Received: 25 August 2023 | Revised: 7 February 2024 | Accepted: 9 February 2024

DOI: 10.1111/iwj.14811

ORIGINAL ARTICLE

IWJ WILEY

A standardized wound infection model for antimicrobial testing of wound dressings in vitro

Cornelia Wiegand[1] | **Sarah Fink**[1] | **Diana C. Mogrovejo**[2] | **Marina Ruhlandt**[2] | **Vanessa Wiencke**[2] | **Thomas Eberlein**[3] | **Florian H. H. Brill**[2] | **Jörg Tittelbach**[1]

[1]Department of Dermatology, Jena University Hospital, Jena, Germany

[2]Dr. Brill + Partner GmbH, Institute for Hygiene and Microbiology, Hamburg, Germany

[3]WCC Wound Competence Centre, Linz, Austria

Correspondence
Cornelia Wiegand, Department of Dermatology, University Hospital Jena, Am Klinikum 1, 07747 Jena, Germany.
Email: c.wiegand@med.uni-jena.de

Funding information
BMWE (Bundesministerium für Wirtschaft und Energie), Grant/Award Number: 16KN077227

Abstract

To investigate the effectiveness of antimicrobial agents against wound infections, experiments using either 2D cultures with planktonic microorganisms or animal infection models are frequently carried out. However, the transferability of the results to human skin is limited by the lack of complexity of the 2D models or by the poor translation of the results from animal models. Hence, there is a need for wound infection models capable of assessing antimicrobial agents. In this study, an easily standardized wound infection model was established. This model consists of a mechanically wounded human skin model on a collagen matrix infected with various clinically relevant bacteria. Infection of the model led to recognition of the pathogens and induction of an inflammatory response. The untreated infection spread over time, causing significant tissue damage. By applying an antimicrobial-releasing wound dressing, the bacterial load could be reduced and the success of the treatment could be further measured by a decrease in the inflammatory reaction. In conclusion, this wound infection model can be used to evaluate new antimicrobial therapeutics as well as to study host-pathogen interactions.

KEYWORDS

3D-skin model, *Pseudomonas aeruginosa*, *Staphylococcus aureus*, wound infection

Key Messages

- There is a need for wound infection models capable of assessing antimicrobial agents as the transferability of experiments using either 2D cultures with planktonic microorganisms or animal infection models are limited.
- In this study, an easily standardized wound infection model consisting of a mechanically wounded human skin model on a collagen matrix infected with various clinically relevant bacteria was established.
- Untreated infections led to induction of an inflammatory response following recognition of the pathogens and caused significant tissue damage.
- Treatment with antimicrobial-releasing wound dressings reduced the bacterial load and decreased the inflammatory reaction.

1 | INTRODUCTION

The skin serves as a protective barrier against microbial invasion. A wound facilitates the entry of various opportunistic and pathogen micro-organisms,[1] which can disrupt the wound healing process through toxic by-products and lead to the formation of a chronic wound.[2] Furthermore, many of these microorganisms can become or are already resistant to various antibiotics, which poses a great socioeconomic problem for hospitals.[3] Chronic wounds are often colonized by different kinds of microorganisms, the most prominent being *Staphylococcus aureus* and *Pseudomonas aeruginosa*.[4] *S. aureus* is a gram-positive bacterium and a facultative pathogen, which can cause a wide range of clinical infections.[5] *P. aeruginosa* is a gram-negative bacteria that is a major cause of hospital acquired infections.[6] It is further known that about three quarters of the chronic wound patients are colonized with *S. aureus* and 30% of these isolates were found to be methicillin resistant.[4] Colonization and local infections can be successfully treated with suitable wound therapeutics. The efficacy of these agents is usually assessed with 2D cultures using planktonic microorganisms.[7] However, these methods lack a critical inflammatory immune response.[8] Therefore, antiseptics must be studied with a more complex model capable of mimicking the wound environment. In accordance, animal models are often used as alternative test systems. However, animal skin differs from human skin in terms of structure and immunological response, which makes it difficult to transfer the data to the human system.[9] Human 3D full-skin models are, therefore, a good alternative for antimicrobial tests. They consist of a dermis with fibroblasts and an epidermis with keratinocytes, which form the stratum corneum.[10] After infection, they can be employed to study the interaction of microorganisms with human skin or for testing of skin disinfection efficacy.[11–13] So far, these investigations were performed on intact skin model surfaces and did not include an inflammatory wound environment. Human infection wound models, on the other hand, are scarcely available. In these models, wounds are either generated by thermal injury or by mechanical damage to create cut or stab wounds.[14–16] Yet, wounding is difficult to standardize because the outcome depends on the duration and pressure used by the person performing the procedure.

In this study, a wound infection model that can be easily standardized is presented. It consists of a punched skin model cultivated on a dermal matrix. The wound models were infected with the two clinically relevant bacteria *S. aureus* and *P. aeruginosa*. These infection models were used to assess the effectiveness of a silver-containing as well as a polyhexamethylene biguanide (PHMB)-containing wound dressing. Therefore, several parameters such as microbial count, wound tissue presentation as well as cytokine secretion and gene expression was studied and compared between untreated and silver dressing-treated models.

2 | MATERIALS AND METHODS

2.1 | Preparation of 3D-wound models

Three-dimensional skin models were prepared as previously reported.[12,17] For artificial wounding, the skin models were punched with a 3 mm biopsy punch (pfm medical, Germany). Rat-tail collagen (medrix biomedicals, Germany) mixed with a gel neutralizing solution (medrix biomedicals, Germany) in a ratio of 4:1 was used for the dermal acellular base component providing mechanical stabilization and a wound bed for the cells to re-grow into. After the collagen had solidified, the punched skin model was placed on the top of this dermal base component, creating a model wound with a standardized diameter of 3.2 mm and a depth of approx. 2.5 mm (Figure 1).

2.2 | Microorganism cultures

S. aureus DSM 4910 (DZMZ, Germany) and *P. aeruginosa* DSM 1117 (DZMZ, Germany) were grown on Columbia agar plates (bioMérieux, France). Bacteria were suspended in tryptic soy broth (Oxoid, UK) and cultured overnight at 37°C under vigorous shaking. The bacterial suspension was washed twice in 0.9% NaCl solution and the number of bacteria in the solution was determined by serial dilution followed by plating on Columbia agar. The agar plates were incubated for 24 h at 37°C, the colonies were counted and the microbial count (in colony-forming units/mL) of the bacterial suspension was calculated.

2.3 | Infection of the wound model

The wound models were infected with 10 µL of a 1×10^9 cfu/mL suspension of *S. aureus* or *P. aeruginosa* placed into the centre of the wound (Figure 1). These high infection doses yielded the best reproducibility for establishment of an evenly spread infection over a short period of time. After 24 h at 37°C in an atmosphere of 5% CO_2, the infected wound models were treated with either a silver containing wound dressing (Suprasorb® A + Ag, Lohmann & Rauscher, Germany) or a PHMB containing wound dressing (Suprasorb® X + PHMB, Lohmann & Rauscher, Germany). The wound dressing was cut into shape with a diameter of 11 mm. Infected and untreated

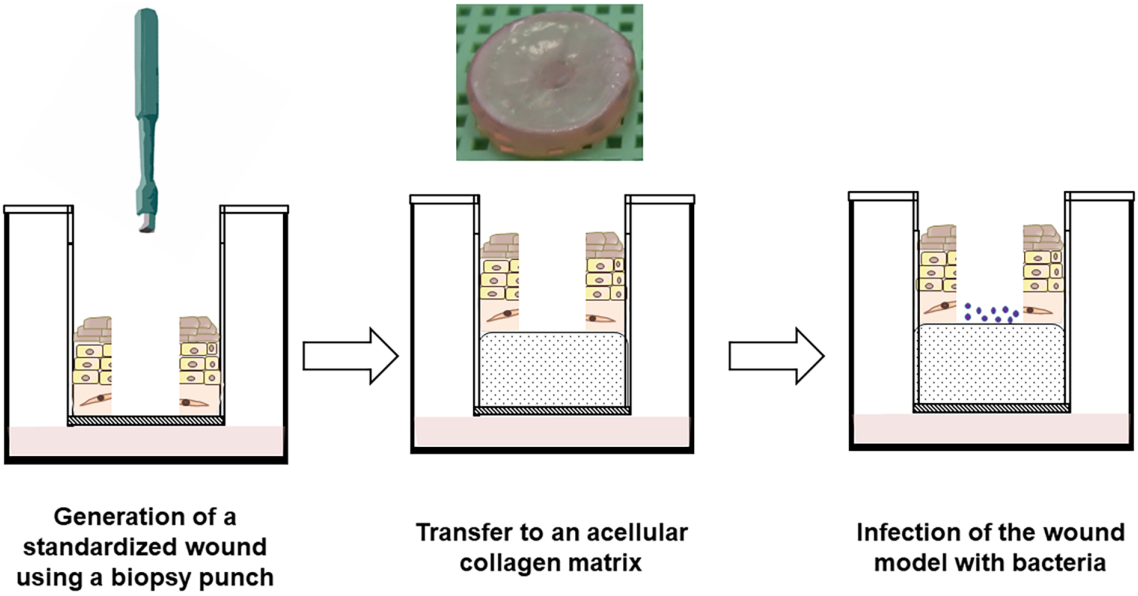

FIGURE 1 Assembling the infected 3D skin wound models: A standardized wound is created with a 3 mm biopsy punch. The wounded model is then transferred to an acellular collagen matrix. Subsequently, the wound is infected with *S. aureus* or *P. aeruginosa*.

wound models served as negative controls. The sampling took place 24 h after the treatment. Supernatants were collected and stored at −20°C for cytokine analysis. For histology, the skin models were transferred to a 4% formalin solution (Dr. K. Hollborn & Söhne, Germany). For gene expression analysis, the skin models were frozen with liquid nitrogen and stored at −80°C.

2.4 | Determination of microbial counts

The microbial load was determined by rinsing the models three times with 1 mL PBS and pooling the rinsing solution for serial dilution. The solution was serially diluted and plated on Columbia agar. The agar plates were incubated for 24 h at 37°C, colonies were counted and the microbial count (in cfu/mL) was calculated.

2.5 | Determination of cytokine levels

Cytokine secretion was quantified using human interleukin (IL)-6 (Mabtech, Sweden), IL-8 and IL-1α (R&D Systems, USA) enzyme-linked immunosorbent assay kits according to the manufacturers' instructions. The optical density was measured at 450 nm with a reference measurement at 620 nm. Interleukin concentrations were calculated according to a standard curve using a 4-parameter fit with lin-log coordinates for optical density. The concentration was expressed as fold secretion and compared to the untreated control.

2.6 | Histological analysis

Formalin-fixed models were progressively dehydrated and embedded in paraffin blocks (Merck, USA) using standard histological protocols. Sections of 4 μ thickness were cut and mounted on object slides. The paraffin contained in the tissue sections was removed by washing in alcohol in descending order prior to staining. Automated deparraffinization and staining with haematoxylin/eosin were performed in the Leica Autostainer XL (Leica, Germany) according to manufacturer's recommendations. The microscopic assessment was carried out using the Keyence digital microscope (Keyence Deutschland GmbH, Germany) and photographs were taken.

2.7 | Visualization of bacterial infection

Microorganisms were visualized in real time using the MolecuLight i:X™ imaging device (MolecuLight Inc., Canada) To do this, the models were irradiated with violet light (405 nm) and presence of bacteria was assessed by auto-fluorescence intensity.[18,19]

2.8 | Determination of gene expression

RNA was isolated using the RNeasy Mini Purification Kit (Qiagen, Germany). cDNA was synthesized using 20 ng of isolated RNA and the High Capacity cDNA Reverse

TABLE 1 Primer sequences used for real-time polymerase chain reaction.

	Primer sequence (5′→ 3′)	
Gene	**Forward primer**	**Reverse primer**
Interleukin-6	CCA CCG GGA ACG AAA GAG AA	GAG AAG GCA ACT GGA CC GAA
Interleukin-8	QT00000322 (Qiagen)	
Interleukin-1α	CGC CAA TGA CTC AGA GGA AGA	AGG GCG TCA TTC AGG ATGAA
Interleukin-23	QT00204078 (Qiagen)	
TNFα	QT00029162	
GM-CSF	TGA ACC TGA GTA GAG ACA CTG C	GCT CCT GGA GGT CAA ACA TTT C
β-actin	QT01680476 (Qiagen)	

Transcription Kit (Thermo Fisher, USA). Real-time-PCR was performed with the QuantiNova SYBR Green PCR Kit (Qiagen, Germany). PCR products were amplified with an initialization step at 95°C for 180 s, followed by 40 cycles at 95°C for 5 s, at 57°C for 10s, and at 72°C for 10 s. The fold change of gene expression was calculated based on the $2^{-\Delta\Delta CT}$ method based on β-actin as housekeeping gene. Primer sequences are listed in Table 1.

2.9 | Statistics

The experiments were performed four times and each measurement was done in four technical replicates ($n = 4$). The evaluation was performed using Excel 2010 (Microsoft Corp., USA) and OriginLab 9.0 (OriginLab Corp., USA). Statistical analyses were performed with SPSS version 27 (IBM Corp., USA). Statistical significance was calculated based on the non-parametric Mann–Whitney *U*-test with $p \leq 0.05$ being considered as statistically significant.

3 | RESULTS

3.1 | Bacterial infection causes tissue damage

The 3D skin models consist of a fully differentiated epidermis, which forms the layers stratum basale, stratum spinosum, stratum granulosum and stratum corneum. Adjacent to the epidermis, a self-produced, thin layer of dermis is visible, which allows the construction of the skin models without the addition of external matrix components. The skin models were injured with a biopsy punch and positioned on an acellular collagen matrix. This procedure enables the creation of a standardized wound depth. The wound models were the infected with *S. aureus* or *P. aeruginosa* (Figure 1). During the first hour after infection, neither structural changes in the skin model occurred nor was the bacterial infection visible. After 24 h, distinct bacterial growth was noticeable by auto-fluorescence measurement (Figure 2A) and in the histological sections (Figure 2B). While *S. aureus* did not elicit visible changes in the skin model morphology during this time, *P. aeruginosa* infection resulted in severe tissue damage and caused a loosening of the skin structure (Figure 2B). The more pronounced effect of *P. aeruginosa* was confirmed by a significantly higher LDH release ($p < 0.05$, Figure 2C), which serves as a marker for cell damage. Nonetheless, *S. aureus* infection also caused a significant rise in LDH levels ($p < 0.05$) in the supernatant after 24 h (Figure 2C). The lesser effect might be explained by the observation that the *S. aureus* infection was first confined to the wound margins and the *P. aeruginosa* infection already had spread throughout the models after 24 h (Figure 2A). Both, *S. aureus* and *P. aeruginosa* infected skin models exhibited extensive tissue damage and dissolution after 48 h, which was already macroscopically visible and featured an even more pronounced bacterial invasion (Figure 2A). Histological assessment corroborated these observations, where the loss of the defined skin structure was found (Figure 2B) and an increase of amounts of bacteria cells was observed. Moreover, tissue damage was verified by significantly increased LDH levels at 48 h after infection with *S. aureus* and *P. aeruginosa* (Figure 2C).

3.2 | Cells exhibit an increased inflammatory response after bacterial infection

Bacterial infection led to an increase of the expression of pro-inflammatory cytokine genes. Despite the slower invasion of *S. aureus* into the wound and later establishment of a fully formed infection compared to *P. aeruginosa*, skin models responded to *S. aureus* with a significant increase in *IL1A* and *TNFA* transcript levels as early as 1 h after infection ($p < 0.05$, Figure 3A). After 24 h, gene expression of *IL6*, *CXCL8*, *IL23* and *GM-CSF* was also found to be significantly induced ($p < 0.05$, Figure 3A).

The upsurge in gene expression after *S. aureus* infection extended beyond 48 h with the exception of IL23, which exhibited a drop in transcript levels at this time. It

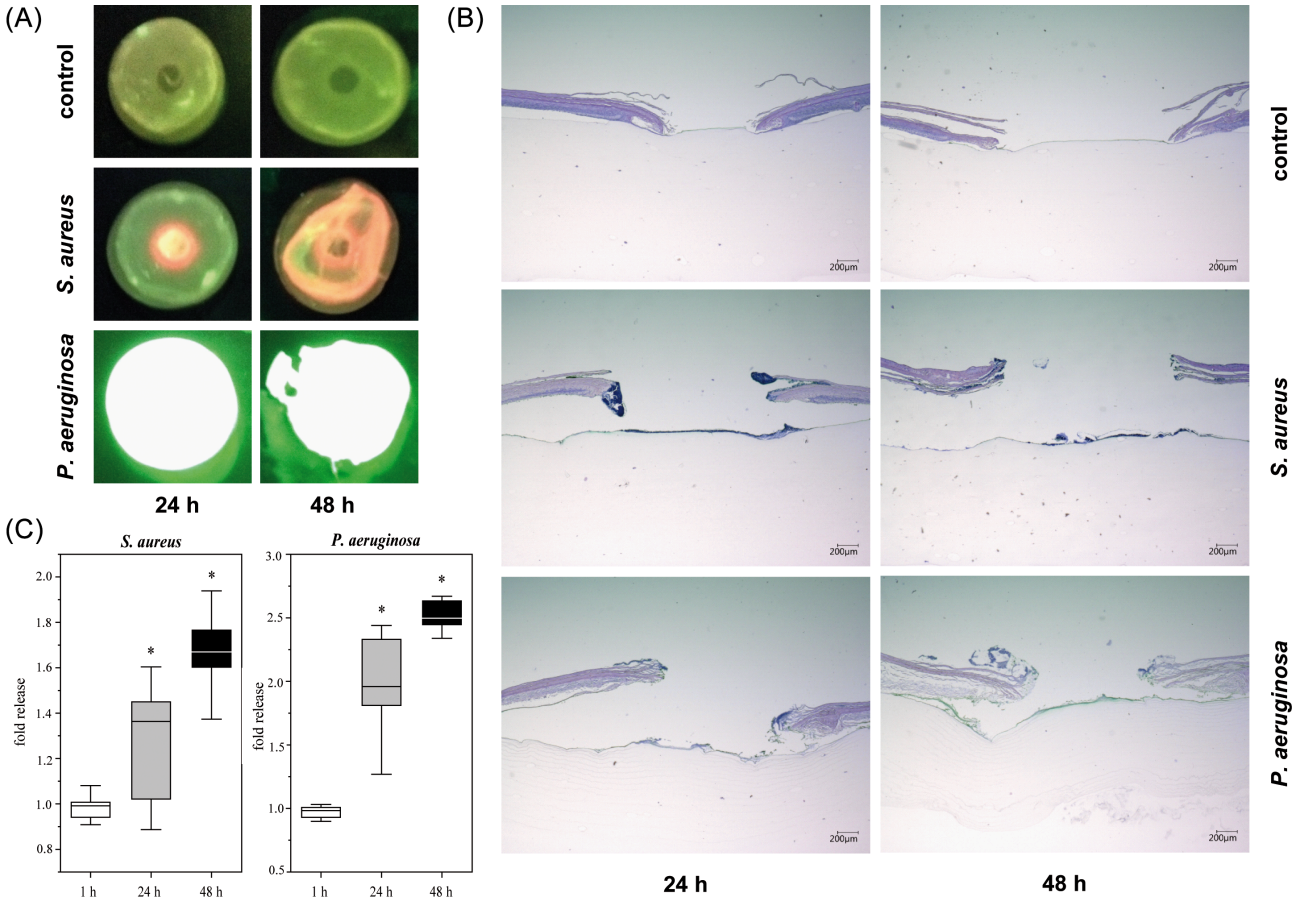

FIGURE 2 Determination of the bacterial effects on the 3D skin wound models: (A) Visualization of bacterial growth using the MolecuLight i:X™ imaging device. The *S. aureus* infection (red fluorescence) was first restricted to the wound margin, whereas *P. aeruginosa* (green fluorescence) rapidly covered the entire model. (B) Histological evaluation of the 3D skin models after infection. Specimens were stained with haematoxylin/eosin. Microbial growth, associated with increasing cell damage and tissue dissolution, was noticed over time. Compared to *S. aureus*, infection with *P. aeruginosa* resulted in significantly earlier and more severe damage. (C) Assessment of cell damage by lactate dehydrogenase (LDH) release. The LDH content was measured in the supernatant of the wound infection models after 1–48 h. Significant cell damage was observed for *S. aureus* after 48 h and for *P. aeruginosa* 24 h after infection notable as a significant increase in release compared to the untreated control. Asterisks indicate significant deviations from the untreated control: $*p < 0.05$.

could further be shown that *S. aureus* did not only lead to a cellular reaction on mRNA levels but the effect was also reflected in a significant secretion of IL-6, IL-8 and IL-1α ($p < 0.05$, Figure 4A). After *P. aeruginosa* infection, a much more pronounced inflammatory response compared to *S. aureus* was noted, which is in accordance with the observed more severe effect of *P. aeruginosa* on the skin models. Already after 1 h, transcript levels of IL1A, TNFA, IL6 and GM-CSF were significantly multiplied ($p < 0.05$, Figure 3B). This process continued over 48 h and ultimately also led to a significant increase of CXCL8 and IL23 gene expression ($p < 0.05$). However, in the case of IL-1A, gene expression was found to be decreased at 48 h after infection corresponding to the decline of skin model viability. Interestingly, the secretion of IL-6 and IL-8 showed a time dependent decrease, while the secretion of IL-1α exhibited a significant rise over time ($p < 0.05$, Figure 4B).

3.3 | Treatment with antimicrobial wound dressing

Twenty four hours after infection, the models were treated with either a silver or PHMB containing wound dressing for 24 h. It could be shown that this antimicrobial intervention led to a significant decrease in *S. aureus* obtainable from the 3d wound models ($p < 0.01$, Figure 5A) as well as reduced *P. aeruginosa* occurrence ($p < 0.05$, Figure 5A). Fluorescence imaging clearly confirmed these results for *S. aureus*, which exhibited a distinct decrease after treatment, whereas in the case of *P. aeruginosa* infection an apparent fluorescence signal was still notable despite the reduced microbial burden (Figure 5B). The histological assessment demonstrated the expected tissue damage after *S. aureus* infection. This effect was not completely reversed during the treatment time of 24 h with the antimicrobial wound dressings, still,

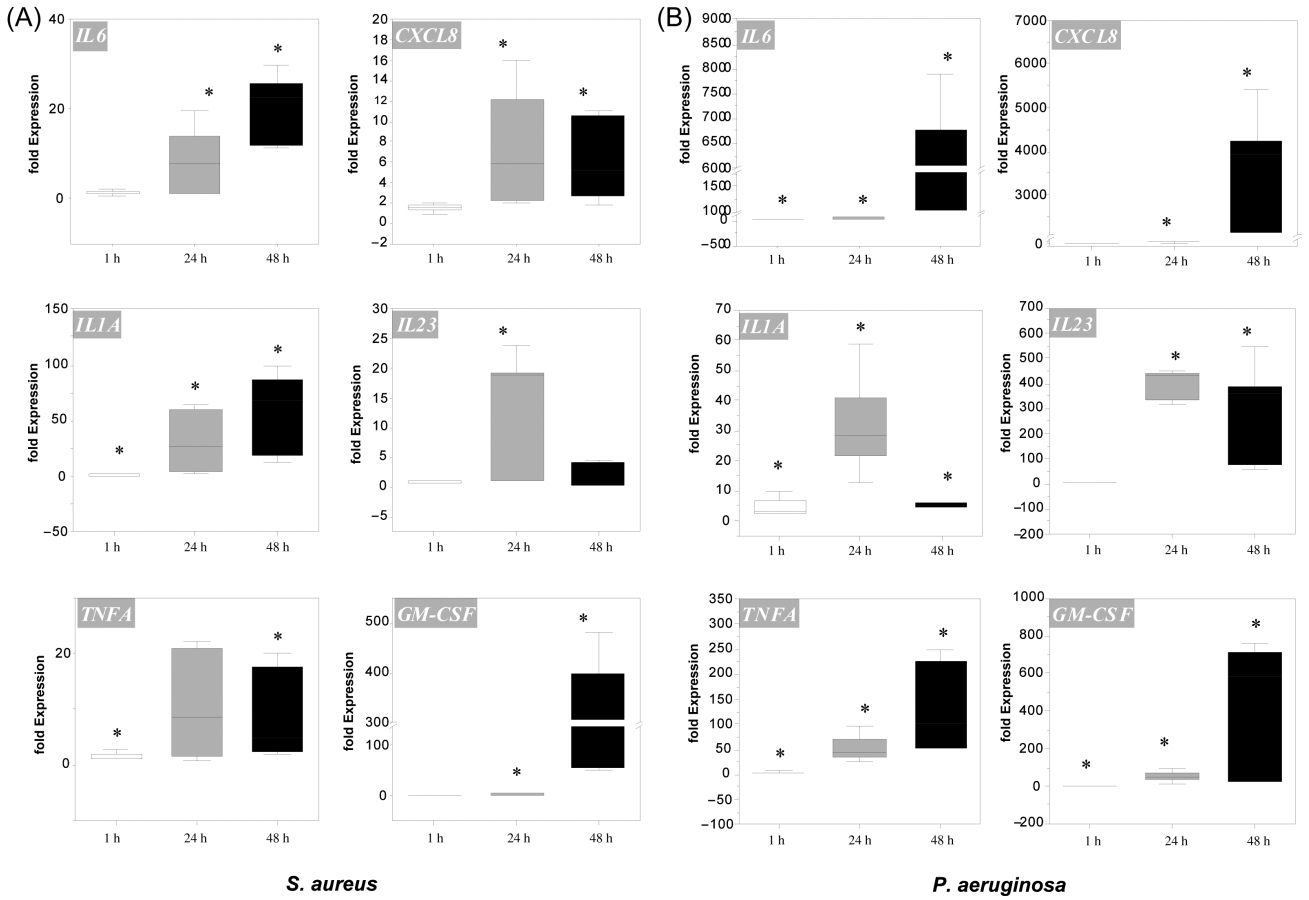

FIGURE 3 Evaluation of inflammatory response after bacterial infection by gene expression analysis: (A) An increase of different pro-inflammatory cytokine gene transcripts was noted after *S. aureus* infection. (B) Cells responded with earlier and partially with higher pro-inflammatory cytokine gene transcripts levels to *P. aeruginosa* infection. The fold expression was calculated compared to the untreated control. Asterisks indicate significant deviations from the respective control: $*p < 0.05$.

a reduction in bacteria at the wound margins was noted (Figure 5C). While a significant decrease of IL-1α secretion under *S. aureus* infection was observed for treatment with the silver dressing ($p < 0.05$), IL-1α release was found to be only slightly reduced with the PHMB dressing (Figure 5D). As anticipated from previous results, infection with *P. aeruginosa* led to even greater tissue damage and dissolution of the skin model, which was also not impeded by treatment with the silver dressing and only to a lesser extend with the PHMB dressing (Figure 5C). Nonetheless, a positive influence on the wound's inflammatory status was noted as treatment with both the silver and the PHMB dressing significantly reduced IL-1α secretion ($p < 0.001$) indicating a positive treatment effect in the direction towards the control of the *P. aeruginosa* infection (Figure 5D).

4 | DISCUSSION

Since 2D-cell cultures or test systems with planktonic microbes cannot embody the complex and inflammatory wound environment, the development of 3D-skin infection wound models represents an alternative way for more realistic examination in a complex environment. There are few wound infection models described in the literature and which the wounds are generated thermally[14] or with the help of a scalpel[15] or cannula.[20] However, a standardized wound is difficult to obtain with these methods because depth and width of the wound are hard to control. Therefore, a standardized wound model with defined wound width and depth was developed in this study. This model was infected with two common wound pathogens. The assessment of the antibacterial effect of either a silver or PHMB containing wound dressing was used to evaluate this model.

Infection of the wound model with *S. aureus* or *P. aeruginosa* resulted in deleterious effects that included dissolution of the tissue structure and secretion of the cytotoxicity marker LDH. *P. aeruginosa* infection caused earlier and more pronounced damage compared to the infection with *S. aureus*. Similar results were reported by Shepard et al. with a skin model infected with various bacteria. Here, *Pseudomonas* also showed a more

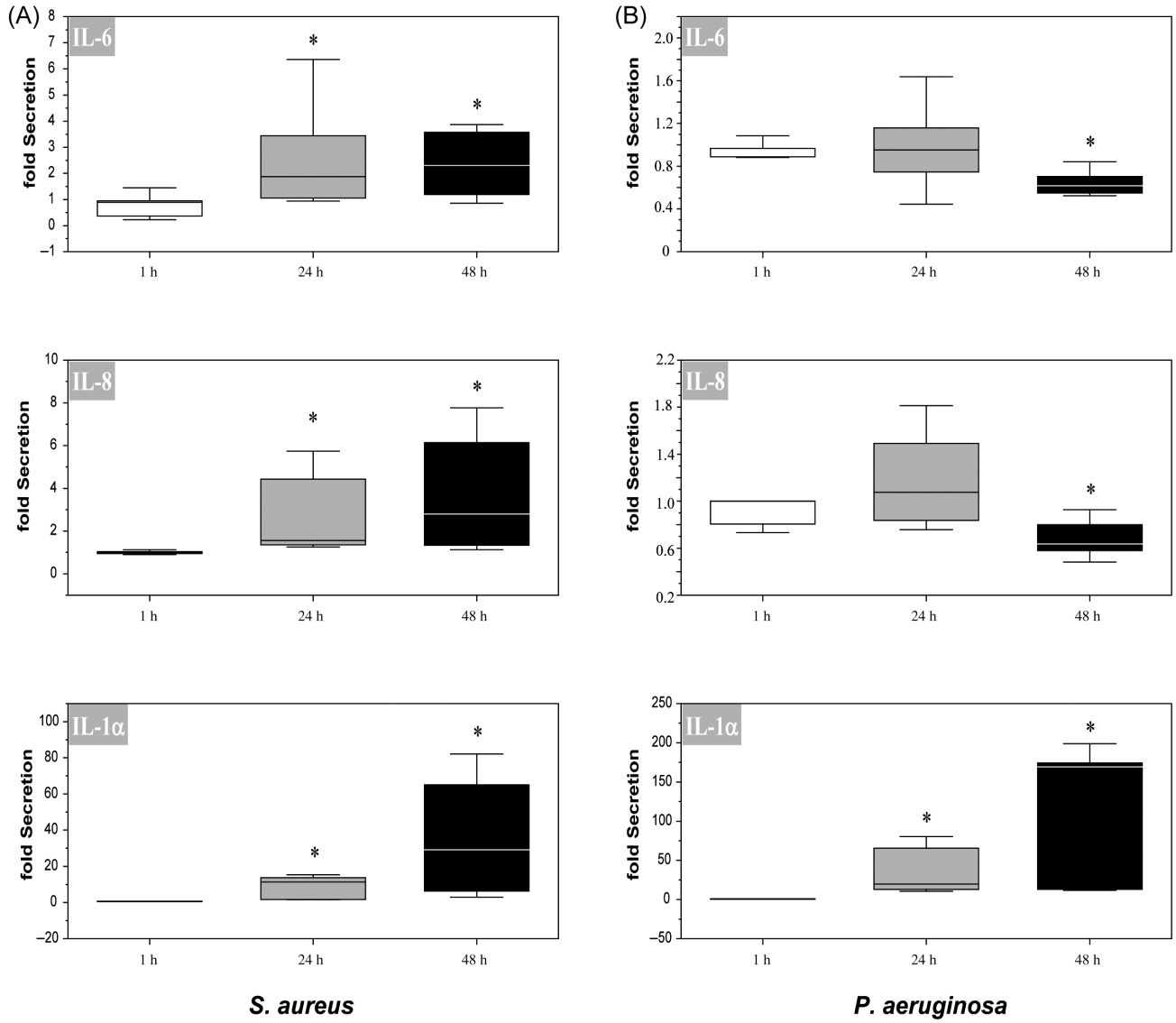

FIGURE 4 Secretion of pro-inflammatory cytokines as response to bacterial infection: (A) A significant increase of pro-inflammatory cytokine release was observed in response to *S. aureus* infection. (B) *P. aeruginosa* infection of the 3D wound models resulted in a decreased liberation of IL-6 and IL-8 and only elicited a significant rise of IL-1α release. Cytokine release was measured by enzyme-linked immunosorbent assay. The fold secretion was calculated compared to the untreated control. Asterisks indicate significant deviations from the respective control: $*p < 0.05$.

destructive effect compared to *S. aureus*. The advance in invasiveness could be due to the release of alkaline proteases and elastase by *Pseudomonas*.[8]

In this study, increased expression and secretion of various pro-inflammatory cytokines were observed. Cytokines are small proteins, secreted by a variety of cells including keratinocytes, fibroblast and macrophages in response to immune stimuli.[21] It was found that infection of the skin models with both bacteria species resulted in an increased gene expression of *IL6, CXCL8, TNFA* and *IL1A*, which is consistent with previous studies using keratinocytes,[22] 3D skin models[11,12] and an infection wound model.[23] However, while the secretion of *S. aureus*-infected wound models increased, infection with *P. aeruginosa* resulted in decreased IL-6 and IL-8 levels. This could be due to the severe damage to the wound models after infection. In contrast, the pro-inflammatory cytokine IL-1α is one of the first secreted cytokines in response to an infection and serves as an alarmin for tissue damage.[24] Biologically active IL-1α is stored by keratinocytes for a rapid immune response. This cytokine is released in the supernatant of the damaged skin models,[25] which explains the increased IL-1α secretion.

GM-CSF transcript levels increased significantly after infection with both bacteria species. This cytokine

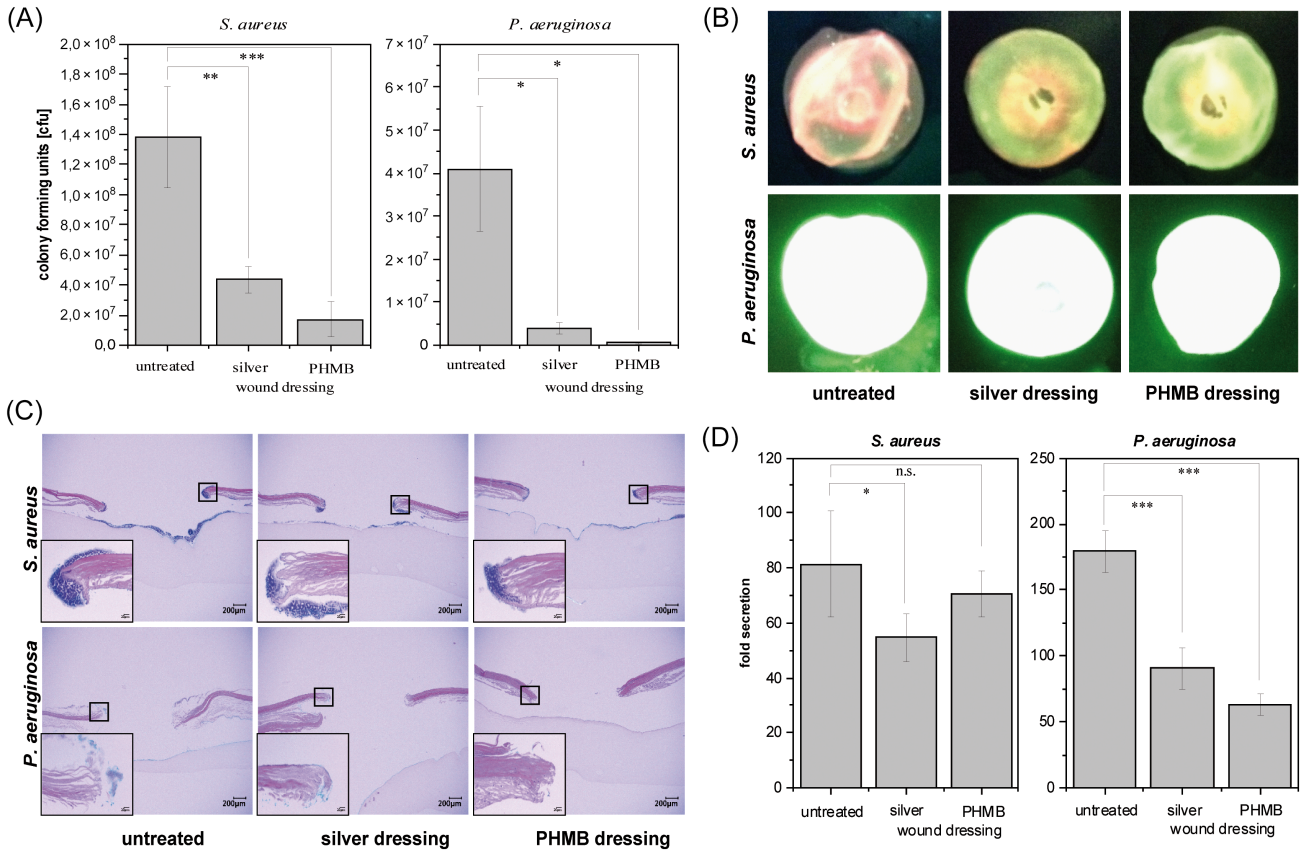

FIGURE 5 Antimicrobial treatment of the infected 3D wound models with a silver-containing wound dressing: (A) Bacteria were quantified after rinsing the models with PBS by plating of serial dilutions on agar plates. The bacterial burden was assessed in relation to the untreated infection control. (B) Visualization of bacterial burden by MolecuLight i:X™ imaging. Treatment with the antimicrobial wound dressings led to a reduction of the red *S. aureus* fluorescence indicating a treatment success compared to the untreated control. In contrast, the cyan fluorescence of *P. aeruginosa* seemed not affected by the antimicrobial treatments. (C) Histological evaluation of the infected wound models with and without antimicrobial treatments. Histological sections were stained with haematoxylin/eosin and photographs were taken at 100-times and 1000-times magnification (insert) using the Keyence digital microscope. Despite a reduction in the bacterial burden through antimicrobial treatment, tissue damage was visible at the endpoint. (D) Determination of IL-1α release after antimicrobial treatments. Reduced IL-1α levels were noted after treatment with the silver-containing wound dressing compared to untreated *S. aureus* and PHMB wound dressing treated wound models. In *P. aeruginosa*-infected wound models, both silver and PHMB wound dressings achieved a significant reduction of IL-1α release. Cytokine secretion was measured by enzyme-linked immunosorbent assay. The fold secretion was calculated compared to the untreated control. Asterisks indicate significant deviations from the respective control: $^{*}p < 0.05$; $^{**}p < 0.01$; $^{***}p < 0.001$.

promotes the activation of immune cells and directs their proliferation.[26] Increased GM-CSF production was also demonstrated by Matsubara et al. in correlation with the presence of *S. aureus* peptidoglycan in human keratinocytes.[27] To the best of our knowledge, this is the first time such an effect is described for skin (wound) models in the presence of *P. aeruginosa*.

IL-23 is a pro-inflammatory cytokine involved in the activation of inflammatory genes and in eliciting type-17 immune responses,[28] which are important for defence against bacteria.[29] Infection of the wound models with *P. aeruginosa* resulted in increased expression of *IL23*. Similar effects were observed in lung infection of mice.[30] However, *S. aureus* infection in our study only caused a transient rise in *IL23* gene expression, an effect observed for the first time in human infection wound models, which is inconsistent with other infection models.[11,12] Yet, Gurjala et al. found, for example, that biofilms of *S. aureus* resulted in a reduced inflammatory response compared to planktonic bacteria in rabbit ear wounds.[31] Since the *S. aureus* strain used in this study is a biofilm former, suppression of *IL-23* gene expression at later time points could explain the effects observed.

For the evaluation of the usability of the wound infection models for assessment of antimicrobial treatments, a silver and a PHMB containing wound dressing were chosen as model therapies. The infected wound models were treated with the antimicrobial wound dressings for 24 h.

In both, *S. aureus* and *P. aeruginosa* infections, antimicrobial treatments resulted in a significant reduction in microorganisms on the 3D skin wound models. In this case, significance of the results is limited, as bacteria were quantified in solution after a washing step, and bacteria that invaded into deeper layers, forming biofilm-like structures that more strongly attach to the wound tissue, would not be regarded. Nonetheless, histological assessment corroborated a reduction in bacteria at the wound margins. Moreover, the results could partially be verified by fluorescence imaging, a quick and non-invasive method for wound infection quantification. Bacteria produce different endogenous fluorophores, which can be visualized by a hand-held fluorescence imaging device when irradiated with violet light (405 nm). For instance, *S. aureus* can be identified by the red fluorescence of porphyrins, natural by-products of bacterial heme production. Cyan-fluorescent pyoverdines are fluorophores specific to pseudomonads.[18] Interestingly, experiments with planktonic *S. aureus*, in contrast to clinical wounds,[19] did not yield a fluorescent signal (own, unpublished data). This confirms the applicability of the present wound infection model. In this study, the reduction for *S. aureus* could be confirmed by the auto-fluorescence images, while the intensity of the fluorescent signal for *P. aeruginosa* remained high. Fluorescent signals from bacteria may persist even after the bacteria themselves have died.[32] Pyoverdines are essential for biofilm formation under iron starved conditions[33] and may have been overproduced here. However, further research needs to be done to elicit the exact mechanism.

Antimicrobial effects of PHMB[34–39] as well as of silver containing wound dressings[40–44] have been widely reported. The cation PHMB interferes with the function of negatively charged phospholipids in the bacterial membranes leading to the loss of membrane integrity, which leads to bacteria cell death.[36] Moreover, it has been shown that PHMB can enter bacteria cells and bind to DNA hindering bacteria progeny.[45] The positively charged silver ions are also able to bind to and penetrate the cell membrane. Interaction with bacterial thiol groups results in inactivation of the respiratory enzymes, inhibition of protein synthesis as well as arrest of bacterial DNA replication.[46] As IL-1α secretion after antimicrobial treatment was only reduced and not completely inhibited, it is likely that treatment with the antimicrobial dressings only led to a decrease of the bacteria numbers, whereas the remaining bacteria and the by-products of bacteria killing were able to trigger an inflammatory reaction. Furthermore, treatment with the dressings failed to completely prevent tissue damage from bacterial invasion. In contrast, Reddersen et al. demonstrated a protective effect of different antimicrobial substances on skin infection models,[12] though in their study the pre-infection time was shorter and the skin models were not previously wounded. Compared to standard in vitro test methods, the antimicrobial effect of the wound dressings in this study appeared to be distinctly lower. For instance, Wiegand et al. reported complete inactivation of *S. aureus* in a co-culture model with HaCaT keratinocytes by the same type of PHMB wound dressing[22] and showed effective killing of *S. aureus* and *P. aeruginosa* by the silver-containing dressing in a standard contact test method.[47] However, these tests used only planktonic bacteria, which are more sensitive to antimicrobial agents. The 3D skin wound models in this study were infected with the microorganisms 24 h prior to antimicrobial treatment, which allows for formation of biofilm-like structures associated with higher antimicrobial tolerance. The latter may very well more effectively mirror the clinical situation. In accordance, the infection wound model described in this study could close the gap between in vitro test procedures and clinical testing.

ACKNOWLEDGEMENTS

The authors would like to thank Denise Rietz for excellent technical support. Open Access funding enabled and organized by Projekt DEAL.

FUNDING INFORMATION

This project (ID 16KN077227) was funded by 'Zentrales Innovationsprogramm Mittelstand (ZIM)' of the BMWE (Bundesministerium für Wirtschaft und Energie).

CONFLICT OF INTEREST STATEMENT

The authors declare no conflicts of interest.

DATA AVAILABILITY STATEMENT

The data that support the findings of this study are available from the corresponding author upon reasonable request.

ORCID

Thomas Eberlein https://orcid.org/0000-0002-0244-0558

REFERENCES

1. Coates M, Blanchard S, MacLeod AS. Innate antimicrobial immunity in the skin: a protective barrier against bacteria, viruses, and fungi. *PLoS Pathog*. 2018;14(12):e1007353.
2. Maheswary T, Nurul AA, Fauzi MB. The insights of microbes' roles in wound healing: a comprehensive review. *Pharmaceutics*. 2021;13(7):981.
3. Avershina E, Shapovalova V, Shipulin G. Fighting antibiotic resistance in hospital-acquired infections: current state and emerging technologies in disease prevention, diagnostics and therapy. *Front Microbiol*. 2021;12:707330.
4. Dissemond J, Schmid EN, Esser S, Witthoff M, Goos M. Bacterial colonization of chronic wounds. Studies on outpatients in a

university dermatology clinic with special consideration of ORSA. *Hautarzt*. 2004;55(3):280-288.
5. Tong SY, Davis JS, Eichenberger E, Holland TL, Fowler VG Jr. *Staphylococcus aureus* infections: epidemiology, pathophysiology, clinical manifestations, and management. *Clin Microbiol Rev*. 2015;28(3):603-661.
6. de Bentzmann S, Plésiat P. The *Pseudomonas aeruginosa* opportunistic pathogen and human infections. *Environ Microbiol*. 2011;13(7):1655-1665.
7. Balouiri M, Sadiki M, Ibnsouda SK. Methods for in vitro evaluating antimicrobial activity: a review. *J Pharm Anal*. 2016;6(2):71-79.
8. Shepherd J, Douglas I, Rimmer S, Swanson L, MacNeil S. Development of three-dimensional tissue-engineered models of bacterial infected human skin wounds. *Tissue Eng Part C Methods*. 2009;15(3):475-484.
9. Robinson NB, Krieger K, Khan FM, et al. The current state of animal models in research: a review. *Int J Surg*. 2019;72:9-13.
10. Randall MJ, Jüngel A, Rimann M, Wuertz-Kozak K. Advances in the biofabrication of 3D skin in vitro: healthy and pathological models. *Front Bioeng Biotechnol*. 2018;6:154.
11. Holland DB, Bojar RA, Farrar MD, Holland KT. Differential innate immune responses of a living skin equivalent model colonized by *Staphylococcus epidermidis* or *Staphylococcus aureus*. *FEMS Microbiol Lett*. 2009;290(2):149-155.
12. Reddersen K, Wiegand C, Elsner P, Hipler UC. Three-dimensional human skin model infected with *Staphylococcus aureus* as a tool for evaluation of bioactivity and biocompatibility of antiseptics. *Int J Antimicrob Agents*. 2019;54(3):283-291.
13. de Breij A, Haisma EM, Rietveld M, et al. Three-dimensional human skin equivalent as a tool to study *Acinetobacter baumannii* colonization. *Antimicrob Agents Chemother*. 2012;56(5):2459-2464.
14. Haisma EM, de Breij A, Chan H, et al. LL-37-derived peptides eradicate multidrug-resistant *Staphylococcus aureus* from thermally wounded human skin equivalents. *Antimicrob Agents Chemother*. 2014;58(8):4411-4419.
15. Charles CA, Ricotti CA, Davis SC, Mertz PM, Kirsner RS. Use of tissue-engineered skin to study in vitro biofilm development. *Dermatol Surg*. 2009;35(9):1334-1341.
16. Schaudinn C, Dittmann C, Jurisch J, et al. Development, standardization and testing of a bacterial wound infection model based on ex vivo human skin. *PLoS One*. 2017;12(11):e0186946.
17. Fink S, Sethmann A, Hipler UC, Wiegand C. In vitro investigation of the principle of action of ammonium bituminosulfonate ointments on a 3D skin model. *Eur J Pharm Sci*. 2022;172:106152.
18. Rennie MY, Dunham D, Lindvere-Teene L, Raizman R, Hill R, Linden R. Understanding real-time fluorescence signals from bacteria and wound tissues observed with the MolecuLight i:X™. *Diagnostics (Basel)*. 2019;9(1):22.
19. Rennie MY, Lindvere-Teene L, Tapang K, Linden R. Point-of-care fluorescence imaging predicts the presence of pathogenic bacteria in wounds: a clinical study. *J Wound Care*. 2017;26(8):452-460.
20. Ku JWK, Marsh ST, Nai MH, et al. Skin models for cutaneous melioidosis reveal Burkholderia infection dynamics at wound's edge with inflammasome activation, keratinocyte extrusion and epidermal detachment. *Emerg Microbes Infect*. 2021;10(1):2326-2339.
21. Coondoo A. The role of cytokines in the pathomechanism of cutaneous disorders. *Indian J Dermatol*. 2012;57(2):90-96.
22. Wiegand C, Abel M, Ruth P, Hipler UC. HaCaT keratinocytes in co-culture with *Staphylococcus aureus* can be protected from bacterial damage by polihexanide. *Wound Repair Regen*. 2009;17(5):730-738.
23. Haisma EM, Rietveld MH, de Breij A, van Dissel JT, El Ghalbzouri A, Nibbering PH. Inflammatory and antimicrobial responses to methicillin-resistant *Staphylococcus aureus* in an in vitro wound infection model. *PloS One*. 2013;8(12):e82800.
24. Dinarello CA. Overview of the IL-1 family in innate inflammation and acquired immunity. *Immunol Rev*. 2018;281(1):8-27.
25. Hill PB, Imai A. The immunopathogenesis of staphylococcal skin infections – a review. *Comp Immunol Microbiol Infect Dis*. 2016;49:8-28.
26. Freund M, Kleine HD. The role of GM-CSF in infection. *Infection*. 1992;20(Suppl 2):S84-S92.
27. Matsubara M, Harada D, Manabe H, Hasegawa K. *Staphylococcus aureus* peptidoglycan stimulates granulocyte macrophage colony-stimulating factor production from human epidermal keratinocytes via mitogen-activated protein kinases. *FEBS Lett*. 2004;566(1–3):195-200.
28. Łukasik Z, Gracey E, Venken K, Ritchlin C, Elewaut D. Crossing the boundaries: IL-23 and its role in linking inflammation of the skin, gut and joints. *Rheumatology (Oxford)*. 2021;60-(Suppl 4):iv16-iv27.
29. Cua DJ, Tato CM. Innate IL-17-producing cells: the sentinels of the immune system. *Nat Rev Immunol*. 2010;10(7):479-489.
30. Dubin PJ, Kolls JK. IL-23 mediates inflammatory responses to mucoid *Pseudomonas aeruginosa* lung infection in mice. *Am J Physiol Lung Cell Mol Physiol*. 2007;292(2):L519-L528.
31. Gurjala AN, Geringer MR, Seth AK, et al. Development of a novel, highly quantitative in vivo model for the study of biofilm-impaired cutaneous wound healing. *Wound Repair Regen*. 2011;19(3):400-410.
32. Kumar NG, Nieto V, Kroken AR, et al. *Pseudomonas aeruginosa* can diversify after host cell invasion to establish multiple intracellular niches. *MBio*. 2022;13(6):e0274222.
33. Banin E, Vasil ML, Greenberg EP. Iron and *Pseudomonas aeruginosa* biofilm formation. *Proc Natl Acad Sci U S A*. 2005;102(31):11076-11081.
34. Lenselink E, Andriessen A. A cohort study on the efficacy of a polyhexanide-containing biocellulose dressing in the treatment of biofilms in wounds. *J Wound Care*. 2011;20(11):534-539.
35. Davis SC, Harding A, Gil J, et al. Effectiveness of a polyhexanide irrigation solution on methicillin-resistant *Staphylococcus aureus* biofilms in a porcine wound model. *Int Wound J*. 2017;14(6):937-944.
36. Hübner NO, Kramer A. Review on the efficacy, safety and clinical applications of polihexanide, a modern wound antiseptic. *Skin Pharmacol Physiol*. 2010;23(Suppl):17-27.
37. Tahir S, Malone M, Hu H, Deva A, Vickery K. The effect of negative pressure wound therapy with and without instillation on mature biofilms in vitro. *Materials (Basel)*. 2018;11(5):811.
38. Schwarzer S, James GA, Goeres D, et al. The efficacy of topical agents used in wounds for managing chronic biofilm infections: a systematic review. *J Infect*. 2020;80(3):261-270.
39. Kramer A, Dissemond J, Kim S, et al. Consensus on wound antisepsis: update 2018. *Skin Pharmacol Physiol*. 2018;31(1):28-58.

40. Kostenko V, Lyczak J, Turner K, Martinuzzi RJ. Impact of silver-containing wound dressings on bacterial biofilm viability and susceptibility to antibiotics during prolonged treatment. *Antimicrob Agents Chemother*. 2010;54(12):5120-5131.
41. Bowler PG, Parsons D. Combatting wound biofilm and recalcitrance with a novel anti-biofilm Hydrofiber® wound dressing. *Wound Med*. 2016;14:6-11.
42. Hill KE, Malic S, McKee R, et al. An in vitro model of chronic wound biofilms to test wound dressings and assess antimicrobial susceptibilities. *J Antimicrob Chemother*. 2010;65(6):1195-1206.
43. Stuermer EK, Plattfaut I, Dietrich M, et al. In vitro activity of antimicrobial wound dressings on *P. aeruginosa* wound biofilm. *Front Microbiol*. 2021;12:664030.
44. Ammons MC, Ward LS, James GA. Anti-biofilm efficacy of a lactoferrin/xylitol wound hydrogel used in combination with silver wound dressings. *Int Wound J*. 2011;8(3):268-273.
45. Chindera K, Mahato M, Sharma AK, et al. The antimicrobial polymer PHMB enters cells and selectively condenses bacterial chromosomes. *Sci Rep*. 2016;6:23121.
46. Halstead FD, Rauf M, Bamford A, et al. Antimicrobial dressings: comparison of the ability of a panel of dressings to prevent biofilm formation by key burn wound pathogens. *Burns*. 2015;41(8):1683-1694.
47. Wiegand C, Heinze T, Hipler UC. Comparative in vitro study on cytotoxicity, antimicrobial activity, and binding capacity for pathophysiological factors in chronic wounds of alginate and silver-containing alginate. *Wound Repair Regen*. 2009;17(4):511-521.

How to cite this article: Wiegand C, Fink S, Mogrovejo DC, et al. A standardized wound infection model for antimicrobial testing of wound dressings in vitro. *Int Wound J*. 2024;21(3):e14811. doi:10.1111/iwj.14811